Chapter 9

Cryogenics for HL-LHC

L. Tavian, K. Brodzinski, S. Claudet, G. Ferlin,
U. Wagner and R. van Weelderen
CERN, TE Department, Genève 23, CH-1211, Switzerland

The discovery of a Higgs boson at CERN in 2012 is the start of a major program of work to measure this particle's properties with the highest possible precision for testing the validity of the Standard Model and to search for further new physics at the energy frontier. The LHC is in a unique position to pursue this program. Europe's top priority is the exploitation of the full potential of the LHC, including the high-luminosity upgrade of the machine and detectors with an objective to collect ten times more data than in the initial design, by around 2030. To reach this objective, the LHC cryogenic system must be upgraded to withstand higher beam current and higher luminosity at top energy while keeping the same operation availability by improving the collimation system and the protection of electronics sensitive to radiation. This chapter will present the conceptual design of the cryogenic system upgrade with recent updates in performance requirements, the corresponding layout and architecture of the system as well as the main technical challenges which have to be met in the coming years.

1. Introduction

The upgrade of the cryogenics for HL-LHC will consist of:

- The design and installation of two new cryogenic plants at P1 and P5 for the high luminosity insertions. This upgrade will be based on a new sectorization scheme aiming at separating the cooling of magnets in this insertion regions form magnets of the arcs as well as on a new cryogenic architecture based on electrical feed boxes located at ground level and vertical superconducting links.
- The design and installation of a new cryogenic plant at P4 for SRF cryo-modules.
- The design of new cryogenic circuits at P7 for HTS links and displaced current feed boxes.

- Cryogenic design support for cryo-collimators and 11 T dipoles at P2, P7 and, if needed, also at P3, P5 and P7.

Figure 1 shows the overall LHC cryogenic layout including the upgraded infrastructure.

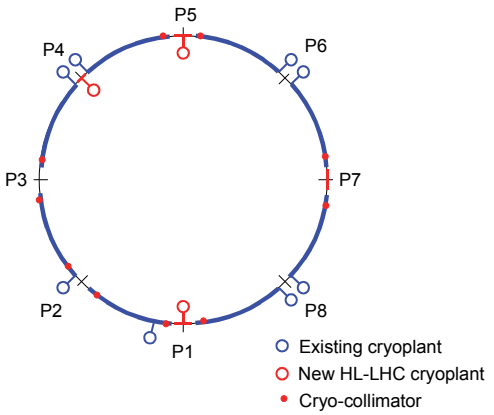

Fig. 1. Overall LHC cryogenic layout including the upgraded infrastructure.

Table 1. LHC upgraded beam parameters for 25-ns bunch spacing.

Parameter		Nominal	Upgrade
Beam energy, E	[TeV]	7	7
Bunch population, N_b	[protons/bunch]	$1.15 \cdot 10^{11}$	$2.2 \cdot 10^{11}$
Number of bunches per beam, n_b	[–]	2808	2808
Luminosity, L	[$cm^{-2}s^{-1}$]	10^{34}	$5 \cdot 10^{34}$
Bunch length	[ns]	1	1

2. LHC Machine Upgrades

2.1. *Upgraded beam parameters and constraints*

The main parameters impacting on the cryogenic system are given in Table 1. With respect to the nominal beam parameters, the beam bunch population will be double and the luminosity in the detectors of the high-luminosity insertions at Points 1 and 5 will be multiplied by a factor of 5.

These upgraded beam parameters will add new constraints on to the cryogenic system:

- The collimation scheme must be upgraded by adding collimators in particular in the continuous cryostat close to Points 2 and 7, and may be also at P3, P1 and P5. The corresponding integration space must be created by developing shorter but stronger 11-T cryo-dipoles. As the new collimators will work at room temperature, cryogenic bypasses are required to guarantee the continuity of the cryogenic and electrical distribution. Figure 2 shows the nominal and upgraded layouts of the continuous cryostat. Halo control for HL-LHC may also require the installation of hollow electron lenses at Point 4, making use of a superconducting solenoid. While not yet in the HL-LHC baseline, this device may be the best option for controlling particle diffusion speed within and depopulating the halo of the high-power hadron beams, avoiding uncontrolled sudden losses during critical operations, like squeezing for putting beam in collision. Figure 3 shows the nominal and upgraded layouts of the Point 4 insertion region, considering the installation of e-lens and of a new SC RF system.
- The increase of the level of radiation to electronics in the tunnel will require relocating power convertors and related current feed boxes in an access gallery at Point 7 and at ground level at Points 1 and 5. New superconducting links will be required to connect the displaced current feed boxes to the magnets. Figures 4 and 5 shows the nominal and upgraded layouts of the insertion regions at Points 1, 5 and 7.
- To better control the bunch longitudinal profile, reduce heating and improve the pile-up density, new cryo-modules of 800-MHz RF cavities will be added to the existing 400-MHz cryo-modules at Point 4 creating a high-harmonic RF system (see Fig. 3). Actually, discussions are under way if a better scheme

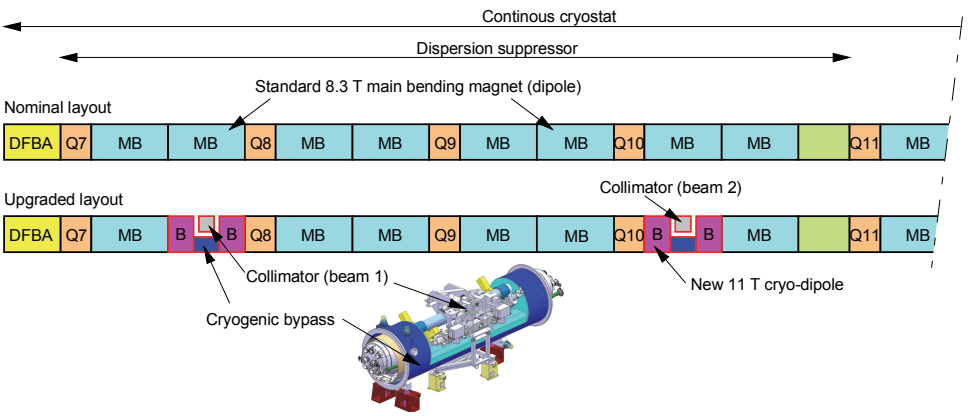

Fig. 2. Upgraded layout of the continuous cryostat (at Points 1, 2, 5 and 7).

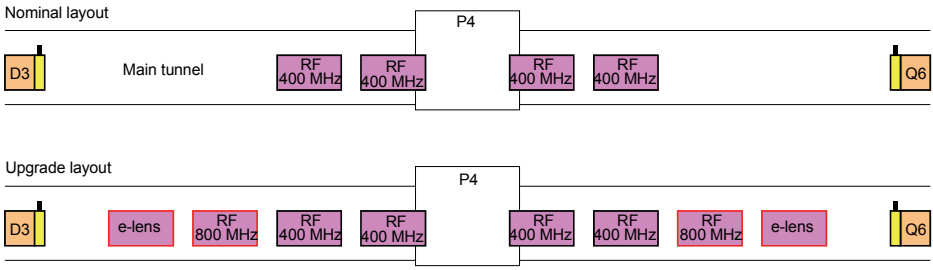

Fig. 3. Upgraded layout of Point 4 insertion region.

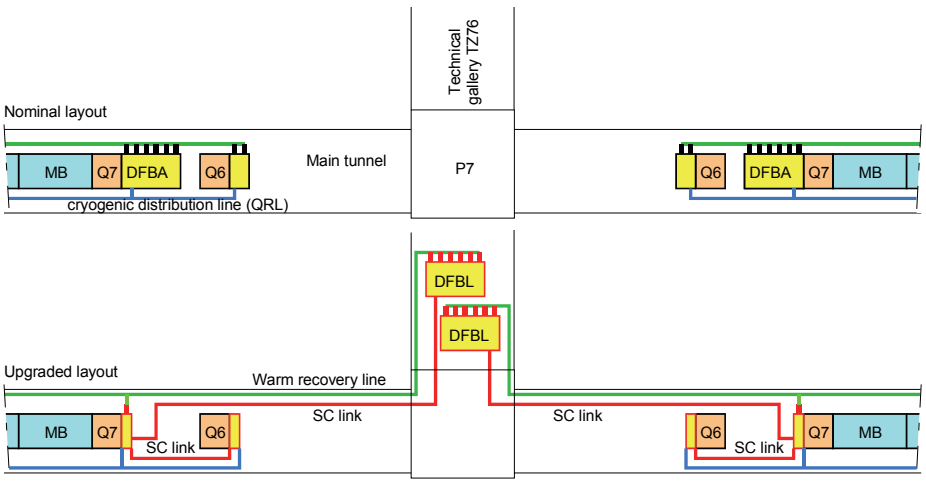

Fig. 4. Upgraded layout of Point 7 insertion region.

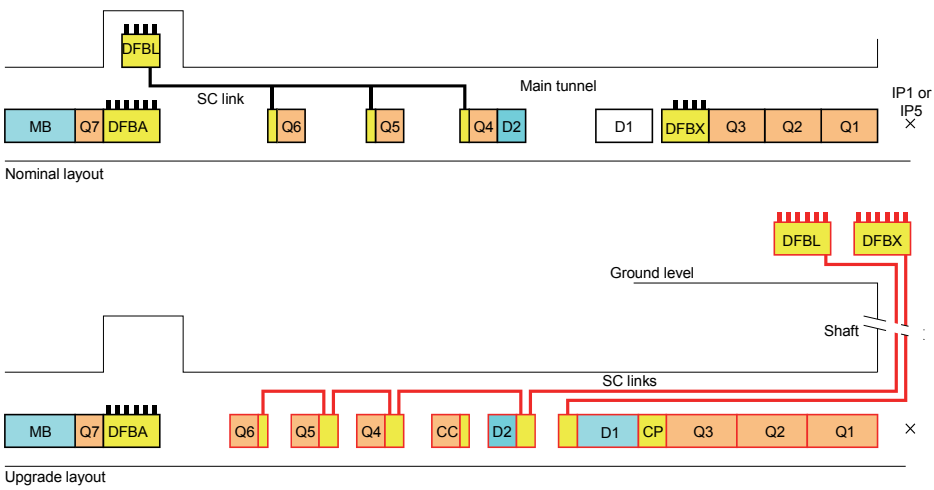

Fig. 5. Upgraded layout of Point 1/5 insertion region (half insertion).

would be installing a new 200-MHz SCRF system, rather than the 800 MHz. However, from the cryogenic point of view the requests are similar, so we will consider in the following text the 800-MHz system that is in an advanced phase of study.

- To improve the luminosity performance, by recovering the geometric luminosity reduction factor (loss of overlap between colliding bunches and increased effective cross-section at the IP) and also possibly to allow the levelling of the luminosity for limiting pile up at the maximum acceptable value for the high-luminosity detectors, cryo-modules of crab cavities (CC) will be added at Points 1 and 5 (see Fig. 5).
- Finally, the matching and final focusing of the beams will require completely new insertions cryo-magnets at Points 1 and 5 (see Fig. 5).

3. Temperature Level and Heat Loads

In Table 2 the static heat inleaks are reported, for the different temperature levels. For new equipment, the thermal performance of supporting systems, radiative insulation and thermal shields is considered identical to the one of existing LHC equipment.

Table 3 gives the dynamic heat loads on the HL-LHC machine. The main concern is the electron-cloud impingement on the beam screens which can only be reduced by an efficient beam scrubbing (dipole off) of the beam screens which is today not demonstrated. Without efficient beam scrubbing (dipole on), the e-cloud activity will remain high (more than 4 W per meter and per beam) in the arcs and dispersion suppressors (DS). This heat deposition corresponds to about

Table 2. Static heat inleaks of HL-LHC machine (w/o contingency).

			Nominal	Upgrade
4.6–20 K	Beam screen circuit (arc + DS)	[mW/m]	140	
	Beam screen circuit (IT)	[mW/m]	125	
	Beam screen circuit (MS)	[mW/m]	578	
1.9 K	Cold mass (arc + DS)	[mW/m]	170	
	Cold mass (IT)	[mW/m]	1250	
	Crab-cavities	[W per module]	0	25
4.5 K	Cold mass (MS)	[mW/m]	3556	
	400 MHz RF module	[W per module]	200	
	800 MHz RF module	[W per module]	0	120
	Electron-lens	[W per module]	0	12
20–300 K	Current lead	[g/s per kA]	0.035	

Table 3. Dynamic heat loads on HL-LHC machine (w/o contingency).

			Nominal	Upgrade
4.6–20 K	Synchrontron radiation (arc + DS)	[mW/m per beam]	165	310
	Image current (arc + DS + MS)	[mW/m per beam]	145	522
	Image current (IT low-luminosity)	[mW/m]	475	1698
	Image current (IT high-luminosity)	[mW/m]	166	596
	E-clouds (arc + DS) (dipole off)	[mW/m per beam]	271	41
	E-clouds (arc + DS) (dipole on)	[mW/m per beam]	4264	4097
	E-clouds (IT high luminosity)	[W per IT]	200	600
	E-clouds (IT low-luminosity)	[W per IT]	200	500
	E-clouds (MS)	[mW/m per beam]	2550	383
	Secondaries (IT beam screen P1 and P5)	[W per IT]	0	650
1.9 K	Beam gas scattering	[mW/m per beam]	24	45
	Resistive heating in splices	[mW/m]	56	56
	Secondaries (IT cold mass P1 and P5)	[W per IT]	155	630
	Secondaries (DS cold mass P1 and P5)	[W per DS]	37	185
	Qrf crab-cavities	[W per module]	0	24
4.5 K	Qrf 400 MHz	[W per module]	101	366
	Qrf 800 MHz	[W per module]	0	183
	E-lens	[W per module]	0	2
20–300 K	Current lead	[g/s per kA]	0.035	

twice the local cooling limitation given by the hydraulic impedance of the beam screen cooling circuits. In addition, the corresponding integrated power over a sector (more than 25 kW) is not compatible with the installed capacity of the sector cryogenic plants. For e-cloud deposition in the arcs and dispersion suppressors, efficient (dipole off) or inefficient (dipole on) beam scrubbing is considered.

The beam screens of the new inner triplets at P1 and P5 will be equipped with tungsten shielding which will be able to stop about half of the secondaries particles escaping the high-luminosity detectors. Despite of this shielding the 1.9 K load, i.e. the energy that collision debris deposit onto the magnet coil and cold mass, increases by four times with respect to the nominal LHC case. This W-shielding reduces the overall refrigeration cost and increases the lifetime of the inner-triplet coils.

4. Impact on Existing Sector Cryogenic Plants

With new cryogenic plants dedicated to the cooling of cryogenic equipment in the P1, P4 and P5 insertions, the cooling duty of the existing sector cryogenic

plants will be reduced and more equally distributed. Figure 6 shows the required cooling capacities for the different temperature levels and compares them to the nominal cooling requirements and to the installed capacities. The low-load sectors equipped with upgraded ex-LEP cryogenic plants have lower installed

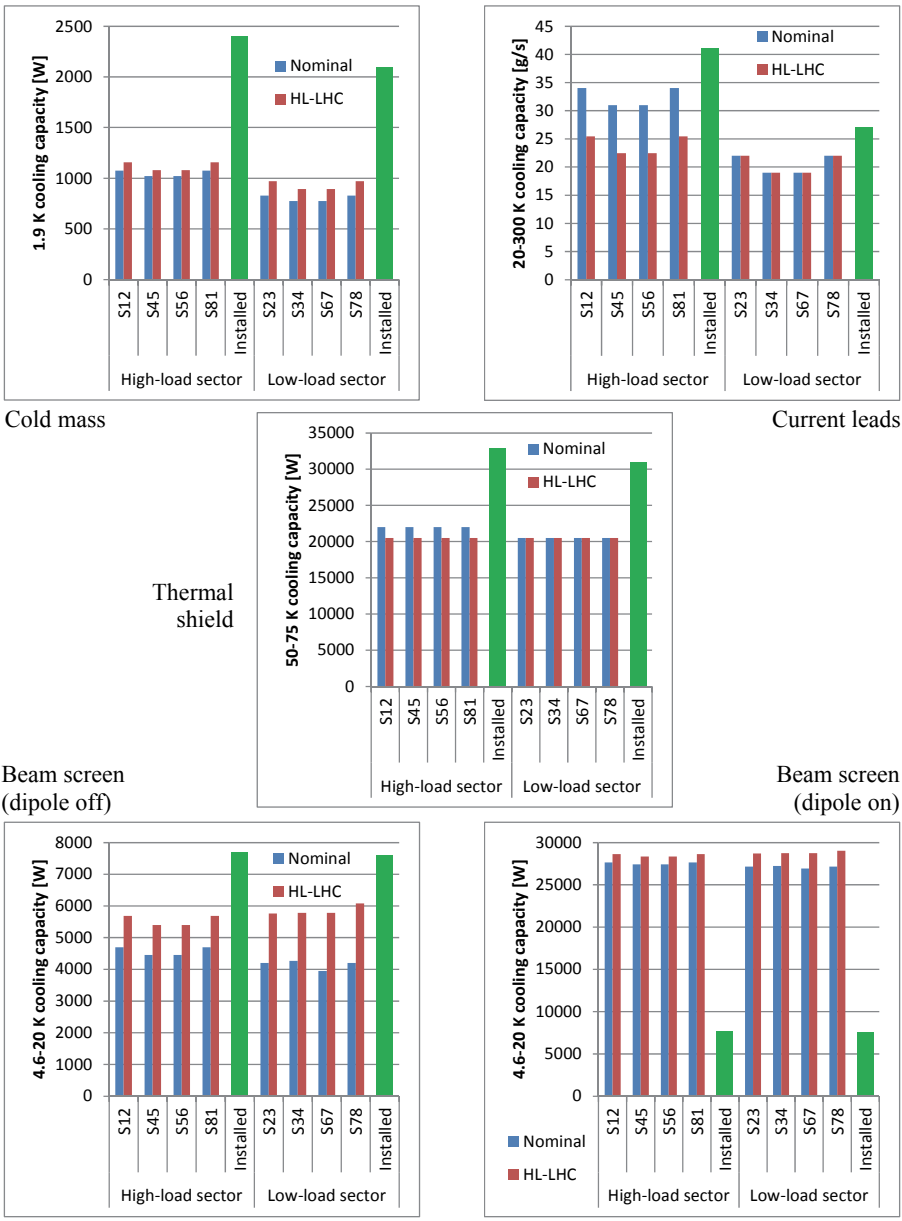

Fig. 6. Cooling capacity requirement of sector cryogenic plants.

capacity than the four cryogenic plants especially ordered for LHC for the high-load sectors. For HL-LHC, sufficient capacity margin still exist providing that the beam scrubbing of dipole beam-screens is efficient (dipole off).

5. New Cryogenics for P4 Insertion

Figure 7 shows the cryogenic architecture of the P4 insertion consisting of:

- a warm compressor station (WCS) located in a noise-insulated surface building and connected to a helium buffer storage;
- a lower cold box (LCB) located in the UX45 cavern and connected to a cryogenic distribution valve box (DVB) as well located in the UX45 cavern;
- main cryogenic distribution lines connecting the cryo-modules to the distribution valve box;
- auxiliary cryogenic distribution lines interconnecting the new infrastructure with the existing QRL service modules (SM) and allowing redundancy cooling with adjacent-sector cryogenic plants;
- a warm-helium recovery line network.

Concerning the installed capacity ($Q_{\text{installed}}$) of the new cryogenic plant, some uncertainty (f_{u}) and overcapacity (f_{o}) margins have to be introduced in the following equation:

- $Q_{\text{installed}} = f_{\text{o}} \times (Q_{\text{static}} \times f_{\text{u}} + Q_{\text{dynamic}})$ with $f_{\text{o}} = 1.5$ and $f_{\text{u}} = 1.5$.

Table 4 gives the installed capacity of the P4 cryogenic plant required at the different temperature levels. The P4 cryogenic plant will require an equivalent capacity of about 6 kW at 4.5 K.

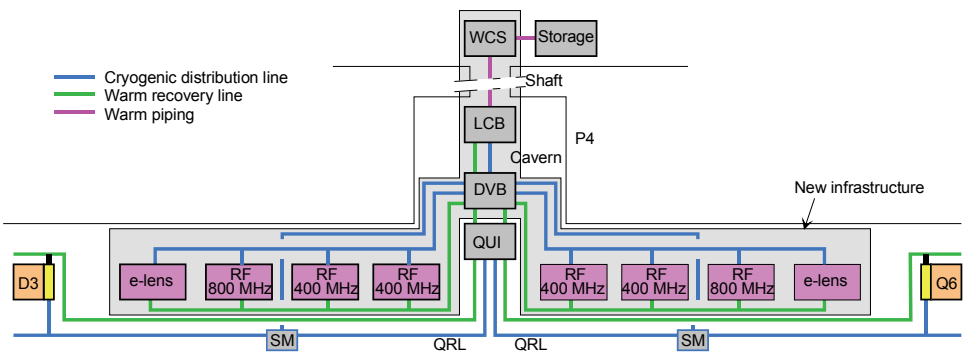

Fig. 7. Upgraded cryogenic architecture at P4.

Table 4. Installed capacity requirements of the new cryogenic plant at P4.

Temperature level		Static	Dynamic	Installed	Equivalent installed capacity @ 4.5 K [kW]	
4.5 K	[W]	1144	1736	5223	5.6	5.8
50–75 K	[W]	1000	0	2250	0.2	

6. New Cryogenics for High-Luminosity Insertions at P1 and P5

Figure 8 shows the cryogenic architecture of the P1 and P5 high-luminosity insertions consisting of:

- a warm compressor station (WCS) located in a noise-insulated surface building and connected to a helium buffer storage;
- an upper cold box (UCB) located in a ground level building;
- a quench buffer (QV) located at ground level;
- one or two cold compressor boxes (CCB) in underground cavern;
- two main cryogenic distribution lines (one per half-insertion);
- two interconnection valve boxes with existing QRL cryogenic line allowing redundancy with the cryogenic plants of adjacent sectors.

Table 5 gives the installed capacity of the P1 and P5 cryogenic plants required at the different temperature levels and using the same uncertainty and overcapacity margins than for P4. The cryogenic plants will require an equivalent capacity of about 18 kW at 4.5 K, including 3 kW at 1.8 K.

At P1 and P5, the superconducting magnets of the ATLAS and CMS detectors are cooled with dedicated cryogenic plants. A possible redundancy with detector cryogenic plants could be interesting in case of major breakdown of the detector cryogenic plants. The corresponding power requirements are about 1.5 kW at 4.5 K for CMS and 3 kW at 4.5 K for ATLAS.

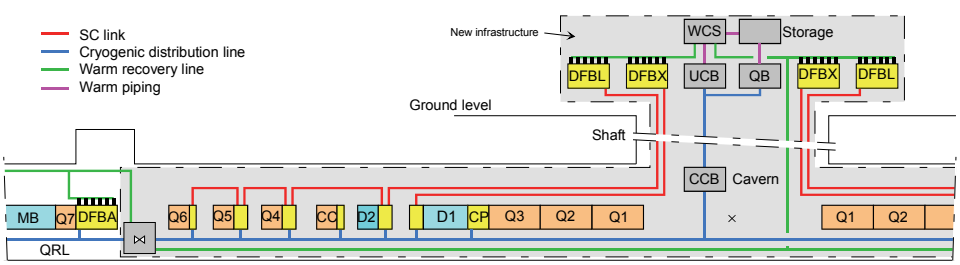

Fig. 8. Upgraded cryogenic architecture at P1 and P5.

Table 5. Installed capacity requirements of the new cryogenic plants at P1 and P5.

Temperature level		Static	Dynamic	Installed	Equivalent installed capacity @ 4.5 K [kW]	
1.9 K	[W]	433	1380	3045	12	
4.5 K	[W]	196	8	452	0.5	
4.6–20 K	[W]	154	2668	4348	2.4	18
50–75 K	[W]	4900	0	7350	0.5	
20–300 K	[g/s]	16	16	59	2.6	

The cooling capacity of 3 kW at 1.8 K is higher than the 2.4-kW installed capacity of a LHC sector which corresponds to the present state-of-the-art for the cold compressor size. Consequently:

- larger cold compressors have to be studied and developed, or,
- parallel cold compressor trains have to be implemented (one 1.5 kW train per half insertion), or,
- duplication of the first stage of cold compression to keep the machine within the available size.

Table 6. Building and general service requirement.

Cryogenic system			P1 and P5	P4
Warm compressor building	Surface	[m^2]	700	400
	Crane	[t]	20	20
	Electrical power	[MW]	4.6	2.0
	Cooling water	[m^3/h]	540	227
	Compressed air	[Nm^3/h]	30	20
	Ventilation	[kW]	250	100
	Type	[-]	Noise-insulated (~108 dBA)	
Surface "SD" building	Surface	[mxm]	30x10	N/A
	Height	[m]	12	N/A
	Crane	[t]	5	N/A
	Electrical power	[kW]	50	N/A
	Cooling water	[m^3/h]	15	N/A
	Compressed air	[Nm^3/h]	90	N/A
Cavern	Volume	[m^3]	200	300
	Local handling	[t]	2	2
	Electrical power	[kW]	100	20
	Cooling water	[m^3/h]	20	20
	Compressed air	[Nm^3/h]	40	30

7. Building and General Service Requirement

Table 6 gives the buildings and general services at P1, P4 and P5 required by the cryogenic infrastructure. At P4, the required surface and volume for the warm compression station and for the cold box are respectively available in the existing SUH4 building and in the UX45 cavern.

8. Conclusion

The HL-LHC project will require a large cryogenic upgrade with new cryogenics challenges. New cooling circuits must be designed to extract up to 13 W/m on 1.9 K cold-mass superconducting cables while keeping sufficient margin with respect to resistive transition limit, as well as up to 23 W/m on inner-triplet beam-screens with possibly a different operating range (40−60 K) and with a large dynamic range which will require specific cryogenic-plant adaptation studies. New cooling method of HTS links, current feed boxes and crab cavities must be developed and validated. The resistive transition containment and helium recovery via cold buffering must be designed for efficient operation. Concerning cryogenic plants, larger 1.8 K refrigeration capacities beyond the present state-of-the-art must be developed including large capacity (1500/3000 W) sub-cooling heat exchangers. This upgrade will be implemented within to main phases. During the second long shutdown of LHC in 2018–2019 calendar years, the upgrade at Point 7 and Point 4 will be implemented. The remaining part will be implemented during the third long shutdown of LHC in 2023–2025 calendar years.

References

[1] V. Baglin, Ph. Lebrun, L. Tavian and R. van Weelderen, 2012, Cryogenic beam screens for high-energy particle accelerators, in *Proceedings of ICEC24*, Fukuoka, Japan (2012), pp. 629-634.

[2] R. Calaga, Crab cavities for the LHC upgrade, in *Proceedings of the Chamonix 2012 Workshop on LHC Performance*, Chamonix, France (2012).

[3] P. Granieri, L. Hincapié, R. van Weelderen, Heat transfer through the electrical insulation of Nb_3Sn cables, in *Proceedings of MT23*, Boston, USA (2013).

[4] P. Granieri and R. van Weelderen, Deduction of steady-state cable quench limits for various electrical insulation schemes with application to LHC and HL-LHC Magnets, in *Proceedings of MT23*, Boston, USA (2013).

[5] L. Rossi and O. Brüning, High luminosity large hadron collider: A description for the European Strategy Preparatory Group, CERN-ATS-2012-236 (2012).

[6] E. Todesco *et al.*, A first baseline for the magnets in the high-luminosity LHC insertion regions, in *Proceedings of MT23*, Boston, USA (2013).
[7] E. Todesco *et al.*, Design studies for the low-beta quadrupoles for the LHC luminosity upgrade, in *Proceedings of ASC 2012*, Portland, Oregon, USA (2012).